Zirconium Complexes Containing Bidentate Pyrrole Ligands: Synthesis, Structural Characterization, and Ethylene Polymerization

Jui-Hsien Huang,*,† Liang-Sheng Chi,† Ru-Ching Yu,† George J. Jiang,‡ Wei-Ta Yang,‡ Gene-Hsiang Lee,§ and Shie-Ming Peng§

Department of Chemistry, National Changhua University of Education, Changhua, Taiwan 500, Department of Chemistry, Chung Yuan Christian University, Chung-Li, Taiwan 320, and Department of Chemistry, National Taiwan University, Taipei, Taiwan 106

Received March 13, 2001

*Summary: Reactions of $ZrCl_4$ with 2 or 3 equiv of Li[$C_4H_3N(CH_2NMe_2)$-2] in toluene afford $ZrCl_2[C_4H_3N(CH_2NMe_2)$-2]$_2$ (**1**) and $ZrCl[C_4H_3N(CH_2NMe_2)$-2]$_3$ (**2**), respectively. Compounds **1** and **2** are characterized by NMR spectroscopy and single-crystal X-ray diffraction. Compound **1** exists as a six-coordinate octahedral structure with the two NMe_2 units taking trans positions, and the seven-coordinate compound **2** shows a chloride-capped octahedral structure in which three bidentate pyrrole ligands form a pseudo-propeller structure with a δλλ form. A polymerization study shows that compounds **1** and **2** exhibit moderate activity toward ethylene, with compound **2** having higher activity.*

Introduction

Metallocene type single-site catalysts for olefin polymerization have been an intriguing topic in the past decades due to their excellent performance in tailoring special properties as well as the microstructure of polymers.[1] Among the metallocene type catalysts, group 3 and 4 metal complexes containing *ansa*-cyclopentadienyl[2] ligands and CGC[3] (constrained geometry catalysts) have attracted much attention. However, non-Cp type ligands, such as alkoxides,[4] amide,[5] and monoanionic bidentate and tridentate arylamine,[6] have attracted much attention recently. We have been interested in using (2-dimethylaminomethyl)pyrrole[7] as a spectator ligand in accordance with early transition metals[8] and group 13 metals[9] to synthesize a series of mono-, bis-, or tris-bidentate metal complexes. Herein we report the synthesis, structural characterization, and ethylene polymerization of zirconium complexes bearing a substituted pyrrole ligand.

Results and Discussion

Synthesis of $ZrCl_2[C_4H_3N(CH_2NMe_2)$-2]$_2$ (1) and $ZrCl[C_4H_3N(CH_2NMe_2)$-2]$_3$ (2). The syntheses of compounds **1** and **2** are depicted in Scheme 1. Two approaches have been used in synthesizing compound **1**: (i) Treatment of $Zr(NMe_2)_4$ with 2 equiv of H[$C_4H_3N(CH_2NMe_2)$-2] in toluene leads to an amine elimination and the formation of the zirconium diamido compound, $Zr(NMe_2)_2[C_4H_3N(CH_2NMe_2)$-2]$_2$ (**3**). Compound **3** is converted to compound **1** via chlorination by adding 2 equiv of Me_3SiCl.[8a] (ii) Reaction of $ZrCl_4$ with 2 equiv of Li[$C_4H_3N(CH_2NMe_2)$-2] in toluene at −78 °C leads to a metathesis reaction forming a dark brown crystalline solid, compound **1**, after workup and recrystallization from toluene. It is worthy to note that method (ii) is a more direct route than method (i) for obtaining zirconium halide compounds bearing substituted pyrrole ligands. The ^{1}H NMR spectrum of **1** in $CDCl_3$ at room temperature shows that the protons of the methylene and dimethylamine units of [$C_4H_3N(CH_2NMe_2)$-2] are both magnetically equivalent, as evidenced of two singlets observed at δ 4.25 and 2.87, respectively. Reaction of $ZrCl_4$ with 3 equiv of Li[$C_4H_3N(CH_2NMe_2)$-2] under similar conditions affords a dark brown crystalline solid of $ZrCl[C_4H_3N(CH_2NMe_2)$-2]$_3$ (**2**) in 73% yield. The ^{1}H

† National Changhua University of Education.
‡ Chung Yuan Christian University.
§ National Taiwan University.

(1) (a) Brintzinger, H. H.; Fischer, D.; Mülhaupt, R.; Rieger, B.; Waymouth, R. M. *Angew. Chem., Int. Ed. Engl.* **1995**, *34*, 1143. (b) Jordan, R. F. *Adv. Organomet. Chem.* **1991**, *32*, 325. (c) Möhring, P. C.; Coville, N. J. *J. Organomet. Chem.* **1994**, *479*, 1.

(2) (a) Stehling, U.; Diebold, J.; Kirsten, R.; Roll, W.; Brintzinger, H. H.; Jungling, S.; Mülhaupt, R.; Langhauser, F. *Organometallics* **1994**, *13*, 964. (b) Spaleck, W.; Antberg, M.; Rohrmann, J.; Winter, A.; Bachmann, B.; Kiprof, P.; Behm, J.; Herrmann, W. A. *Angew. Chem., Int. Ed. Engl.* **1992**, *31*, 1347. (c) Chacon, S. T.; Coughlin, E. B.; Henling, L. M.; Bercaw, J. E. *J. Organomet. Chem.* **1995**, *497*, 171.

(3) (a) LaPointe, R. E. U.S. Patent No. 5321106, June 14, 1994. (b) Lai, S.; Wilson, J. R.; Knight, G. W.; Stevens, J. C.; Chum, P.-W. U.S. Patent, No. 5272236, December, 1993. (c) Canich, J. A. M. Eur. Pat. App. 90309899.4, September 10, 1990. (d) Devore, D. D.; Timmers, F. J.; Hasha, D. L.; Rosen, R. K.; Marks, T. J.; Deck, P. A.; Stern, C. L. *Organometallics* **1995**, *14*, 3132. (e) Shipiro, P. J.; Bunel, E.; Schaefer, W. P.; Bercaw, J. E. *Organometallics* **1990**, *9*, 867.

(4) (a) Fokken, S.; Spaniol, T. P.; Kang, H.-C.; Massa, W.; Okuda, J. *Organometallics* **1996**, *15*, 5069. (b) Mack, H.; Eisen, M. S. *J. Chem. Soc., Dalton Trans.* **1998**, 17. (c) van der Linden, A.; Schaverien, C. J.; Meijboom, N.; Ganter, C.; Orpen, G. A. *J. Am. Chem. Soc.* **1995**, *117*, 3008.

(5) (a) Scollard, J. D.; McConville, D. H.; Vittal, J. J. *Organometallics* **1997**, *16*, 4415. (b) Baumann, R.; Davis, W. M.; Schrock, R. R. *J. Am. Chem. Soc.* **1997**, *119*, 3830.

(6) (a) Chauhan, M.; Chuit, C.; Corriu, R. J. P.; Mehdi, A.; Reyé, C. *Organometallics* **1996**, *15*, 4326. (b) Jastrzebski, J. T. B. H.; van Koten, G.; Konijn, M.; Stam, C. H. *J. Am. Chem. Soc.* **1982**, *104*, 5490. (c) Abbenhuis, H. C. L.; Rietveld, M. H. P.; Haarman, H. F.; Hogerheide, M. P.; Spek, A. L.; van Koten, G. *Organometallics* **1994**, *13*, 3259. (d) Gossage, R. A.; van de Kuil, L. A.; van Koten, G. *Acc. Chem. Res.* **1998**, *31*, 423. (e) Kamepalli, S.; Carmalt, C. J.; Culp, R. D.; Cowley, A. H.; Jones, R. A. *Inorg. Chem.* **1996**, *35*, 6179.

(7) (a) Herz, W.; Dittmer, K. *J. Am. Chem. Soc.* **1947**, *69*, 1698. (b) Kim, H.; Elsenbaumer, R. L. *Tetrahedron Lett.* **1998**, *39*, 1087.

(8) (a) Huang, J. H.; Kuo, P. C.; Lee, G.-H.; Peng, S. M. *J. Chin. Chem. Soc.* **2000**, *27*, 1191. (b) Huang, J. H.; Chi, L. S.; Huang, F. M.; Kuo, P. C.; Lee, G. H.; Peng, S. M. *J. Chin. Chem. Soc.* **2000**, *27*, 895.

(9) Huang, J. H.; Chen, H. J.; Chang, J. C.; Lee, G. H.; Peng, S. M. *Organometallics,* **2001**, *20*, 2647.

10.1021/om010198b CCC: $20.00
Publication on Web 12/17/2001

Scheme 1

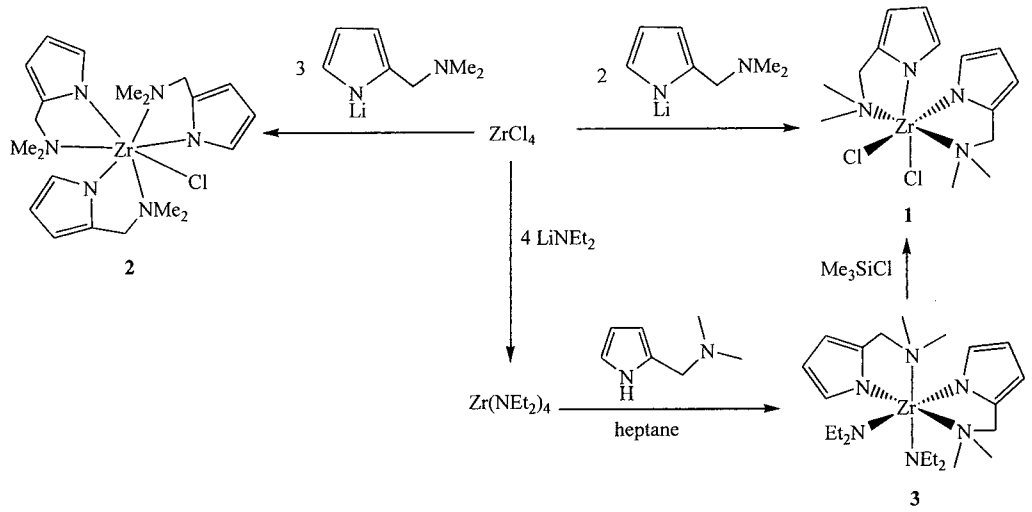

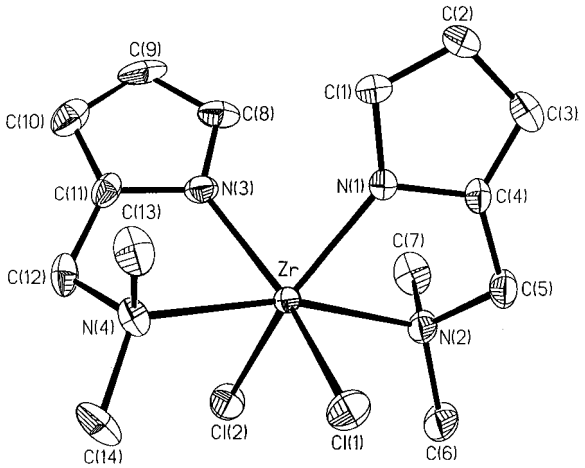

Figure 1. ORTEP plot of compound **1**. Thermal ellipsoids are drawn at 50% probability. Hydrogen atoms are omitted for clarity.

NMR spectrum of **2** in $CDCl_3$ at room temperature reveals that the [$C_4H_3N(CH_2NMe_2)$-2] ligands are magnetically equivalent in that two broad resonances are observed at δ 4.08 and 3.60 for the diastereotopic methylene protons of CH_2N and one broad resonance for the methyl groups of the NMe_2 unit at δ 2.36. A variable-temperature ^1H NMR spectroscopic study reveals that compound **2** exhibits two singlets at δ 2.03 and 2.69 for the NMe_2 unit in $CDCl_3$ at −60 °C. These signals coalescence at ca. 5 °C. The activation energy, $\Delta G^{\ddagger}$, presumably a process involving dissociation/association of the NMe_2 units of compound **2** in solution, is estimated by the slow limit at ca. 12 kcal/mol. **Crystal Structure of $ZrCl_2[C_4H_3N(CH_2NMe_2)$-2]$_2$ (1).** Crystals suitable for X-ray structure analysis were grown from a saturated solution of compound **1** in toluene at −20 °C. The ORTEP drawing of the molecular structure of **1** is shown in Figure 1. The data collection and selected bond distances and angles are shown in Tables 1 and 2, respectively. The geometry around the Zr center is best described as a slightly distorted octahedral with angles N(4)−Zr−N(2), Cl(2)−Zr−N(1), and Cl(1)−Zr-N(3) of 165.25(8)°, 148.40(6)°, and 147.46(6)°, respectively. The two bidentate [$C_4H_3N(CH_2NMe_2)$-2] ligands bound to the Zr center lead to acute bite angles N(3)−Zr−N(4) and Cl(1)−Zr−N(3) of 72.44(9)° and 72.44(8)°, respectively. The average bond distance of Zr−N (pyrrole) is ca. 0.15 Å shorter than that of Zr−N (NMe_2 unit), indicating stronger σ-bonding between the pyrrole and the Zr atom than the bonding of the Me_2N to Zr. It is worthy to note in comparing the molecular structures of **1** and **3** that the two NMe_2 units of compound **1** adopt trans positions while those of compound **3** are arranged in cis positions. One reasonable explanation for the phenomena is the sterical interactions between the NMe_2 units and the diethylamido units.

Table 1. Summary of Crystallographic Data for Compounds 1 and 2

	1	**2**
empirical formula	$C_{14}H_{22}Cl_2N_4Zr$	$C_{21}H_{33}ClN_6Zr$
fw	408.48	496.20
cryst syst	orthorhomic	monoclinic
space group	$Pna2_1$	$P2_1$
a, Å	16.6947(2)	9.7085(2)
b, Å	10.3351(2)	13.6008(3)
c, Å	10.1463(2)	18.1659(4)
β, deg	104.013(1)	
volume, Å^3/Z	1750.66(5)/4	2327.30(9)/4
density(calcd), Mg/m^3	1.550	1.416
abs coeff, mm^{-1}	0.932	0.606
F(000)	832	1032
cryst size, mm	0.22 × 0.20 × 0.18	0.35 × 0.30 × 0.12
θ range for data collection	2.32−27.50°	1.16−27.50°
no. of reflns collected	12 486	15 213
no. of ind reflns	4016 (R_{int} = 0.0395)	10434 (R_{int} = 0.0274)
max. and min. transmn	0.8621 and 0.7798	0.8944 and 0.7419
no. of data/restraints/params	4015/01/191	10432/1/524
goodness-of-fit on F^2	1.042	1.016
final R indices [$I>2\sigma(I)$]	R1 = 0.0284, wR2 = 0.0547	R1 = 0.0335, wR2 = 0.0601
R indices (all data)	R1 = 0.0348, wR2 = 0.0563	R1 = 0.0407, wR2 = 0.0627
abs structure param	−0.04(3)	−0.04(2)
extinction coeff	0.0042(3)	0.0024(2)
largest diff peak and hole, e Å^{-3}	0.314 and −0.255	0.281 and −0.312

Crystal Structure of $ZrCl[C_4H_3N(CH_2NMe_2)$-2]$_3$ (2). Crystals of compound **2** suitable for X-ray structure analyses were grown from a saturated toluene solution at −20 °C. Two independent molecules are found in a unit cell, and the two molecules are very similar. However, only one molecule is described here. The X-ray

Table 2. Selected Bond Distances (Å) and Angles (deg) for Compounds 1 and 2

1

Zr−N(1)	2.140(2)	Zr−N(2)	2.147(2)	Zr−N(2)	2.384(2)
Zr−N(4)	2.403(2)	Zr−Cl(1)	2.4246(6)	Zr−Cl(2)	2.4320(7)
N(1)−Zr−N(3)	82.31(10)	N(1)−Zr−N(2)	72.44(8)	N(3)−Zr−N(2)	119.84(9)
N(1)−Zr−N(4)	119.48(8)	N(3)−Zr−N(4)	72.44(9)	N(2)−Zr−N(4)	165.25(8)
N(1)−Zr−Cl(1)	93.47(7)	N(3)−Zr−Cl(1)	147.46(6)	N(2)−Zr−Cl(1)	88.88(6)
N(4)−Zr−Cl(1)	82.02(6)	N(1)−Zr−Cl(2)	148.40(6)	N(4)−Zr−Cl(2)	88.29(6)
Cl(1)−Zr−Cl(2)	105.95(3)				

2

Zr(1)−N(3)	2.140(2)	Zr(1)−N(5)	2.150(2)	Zr(1)−N(1)	2.189(2)
Zr(1)−Cl(1)	2.4585(8)	Zr(1)−N(2)	2.512(2)	Zr(1)−N(4)	2.552(2)
Zr(1)−N(6)	2.731(3)				
N(3)−Zr(1)−N(5)	108.03(9)		N(3)−Zr(1)−N(1)	84.39(9)	
N(5)−Zr(1)−N(1)	84.83(9)		N(3)−Zr(1)−Cl(1)	114.00(7)	
N(5)−Zr(1)−Cl(1)	117.91(7)		N(1)−Zr(1)−Cl(1)	140.97(6)	
N(3)−Zr(1)−N(2)	82.11(9)		N(5)−Zr(1)−N(2)	152.79(9)	
N(1)−Zr(1)−N(2)	70.80(8)		Cl(1)−Zr(1)−N(2)	77.80(7)	
N(3)−Zr(1)−N(4)	68.06(8)		N(5)−Zr(1)−N(4)	79.16(9)	
N(1)−Zr(1)−N(4)	141.52(8)		Cl(1)−Zr(1)−N(4)	76.76(6)	
N(2)−Zr(1)−N(4)	127.65(8)		N(3)−Zr(1)−N(6)	169.24(9)	
N(5)−Zr(1)−N(6)	69.29(9)		N(1)−Zr(1)−N(6)	84.98(9)	
Cl(1)−Zr(1)−N(6)	75.67(6)		N(2)−Zr(1)−N(6)	95.95(8)	
N(4)−Zr(1)−N(6)	120.43(8)				

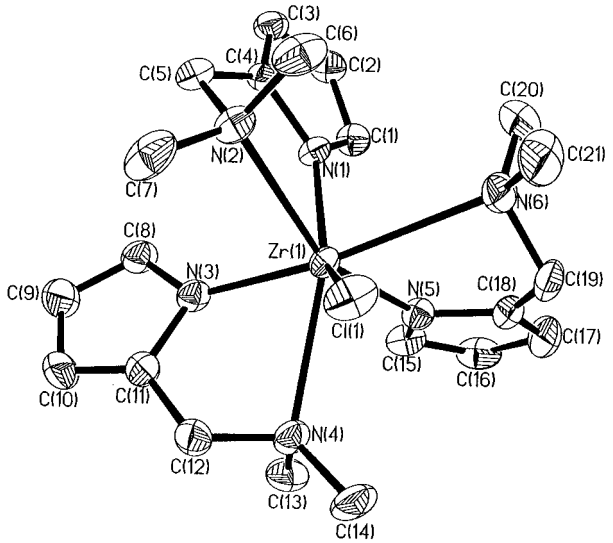

Figure 2. ORTEP plot of compound **2**. Thermal ellipsoids are drawn at 50% probability. Hydrogen atoms are omitted for clarity.

crystallographic data collection and selected bond distances and angles are shown in Tables 1 and 2, respectively. The ORTEP drawing of one of the two independent molecules is depicted in Figure 2. The seven-coordinate compound **2** can be viewed as a chloride-capped octahedron in which the three bidentate pyrrole ligands are arranged in a pseudo-propeller structure. The three bidentate pyrrole ligands bound to the zirconium center form three five-membered rings with a $\delta\lambda\lambda$ arrangement, as shown in Figure 3. By considering the steric and electronic effect, the variations of the molecular structures **1** and **2** can be summarized as follows: (i) the bite angle of [$C_4H_3N(CH_2$-NMe_2)-2] (av 69.41°) in the more sterically congested compound **2** is smaller than that in compound **1** (av 72.44°); (ii) the coordinate NMe_2−Zr bond distance (av 2.60 Å) in the more electron-rich compound **2** is much longer that that in compound **1** (av 2.39 Å), while the Zr−Cl bond distances for both compounds are in the same range (ca. 2.4 Å); (iii) the pyrroles of compound **2** are trans to NMe_2 of the other pyrrole, while one pyrrole of compound **1** is cis to another pyrrole.

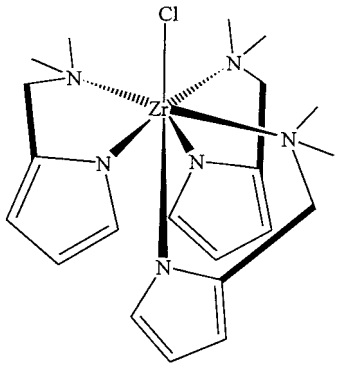

Figure 3. Substituted pyrrole ligand conformation of compound **2**, which is bound to a zirconium atom. The figure shows the three five-membered rings contain the $\delta\lambda\lambda$ form.

Table 3. Data for Ethylene Polymerization[a]

entry	catalyst	temp (°C)	activity (kg mol^{-1} h^{-1})	T_m (°C)	M_w/M_n (PDI)
1	**1**	30	5	136.7	NA[b]
2	**1**	50	5	137.6	NA
3	**1**	70	35	136.7	NA
4	**1**	90	70	136.8	NA
5	**2**	30	15	140.2	NA
6	**2**	50	25	135.5	NA
7	**2**	70	70	134.4	NA
8	**2**	90	175	138.9	1751942/8594 (203.86)

[a] Pressure: 60 psi; catalyst: 2×10^{-6} mol; [MAO]/[Zr] = 1000; reaction time: 1 h. [b] NA, not available due to low yield of the polyethylene.

Ethylene Polymerization. An ethylene polymerization study was carried out using compounds **1** and **2** in toluene. Preliminary results are summarized in Table 3 and have revealed that compounds **1** and **2** exhibit moderate catalytic activities toward ethylene polymerization. Entries 4 and 8 show higher activities than the other entries, indicating the activity of catalysts increases with an increase in reaction temperature. The polydispersity of the polymer produced from **1** was

broad, presumably as a result of the formation of multiple catalyst sites.

Experimental Section

General Procedures. All the reactions were performed using standard Schlenk techniques in an atmosphere of high-purity nitrogen or in a glovebox. Diethyl ether was dried over Na/benzophenone ketyl and distilled before use. (2-Dimethylaminomethyl)pyrrole[7] and its corresponding lithium reagent[8b] were synthesized according to published literature. $ZrCl_4$ and MAO (10 wt % in toluene) were purchased from Aldrich Co. and used as received. Ethylene was obtained from San Fu Chemical Co., Taiwan. $CDCl_3$ was degassed by the freeze-and-thaw method and dried over 4 Å molecular sieves. ^1H and ^{13}C NMR spectra were collected on a Bruker AC200 at room temperature unless noted otherwise. VT NMR spectra were performed with a Varian 600 instrument. Elemental analysis was performed on a Perkin-Elmer CHN-2400. Both compounds are very air-sensitive and readily decompose upon expose to air. The ^1H NMR spectra for compounds **1** and **2** are included in the Supporting Information.

$ZrCl_2[C_4H_3N(CH_2NMe_2)-2]_2$ (1). To a 100 mL Schlenk flask charged with 20 mL of toluene and $ZrCl_4$ (1.0 g, 4.29 mmol) was added dropwise a Li[$C_4H_3N(CH_2NMe_2)$-2] (1.12 g, 8.61 mmol)/toluene (20 mL) suspension at −78 °C with stirring. The mixture was stirred at room temperature for 5 h, and the resulting suspension was filtered through Celite. The filtrate was dried under vacuum to remove the volatiles, and the resulting solid was recrystallized from toluene to generate 1.31 g of **1** in 75% yield. A crystal suitable for X-ray structure analysis was obtained from a saturated toluene solution upon standing at −20 °C for several days. ^1H NMR ($CDCl_3$): 2.87 (s, 12H, N*Me*$_2$), 4.25(s, 4H, C*H*$_2$N), 5.97 (m, 4H), 6.07 (m, 2H). ^{13}C NMR ($CDCl_3$): 47.6 (q, J_{CH}=137 Hz, N*Me*$_2$), 63.2 (t, J_{CH} = 139, *C*H$_2$N), 104.2 (d, J_{CH} = 167 Hz), 108.9 (d, J_{CH} = 168 Hz), 128.3 (d, J_{CH} = 175 Hz), 136.3 (s). Anal. Calcd for $C_{14}H_{22}Cl_2N_4Zr$: C,41.17; H, 5.43; N, 13.72. Found: C, 39.38; H, 5.55; N, 12.21. No satisfactory analyses were obtained due to the air-sensitivity of this compound.

$ZrCl[C_4H_3N(CH_2NMe_2)$-2$]_3$ (2). To a 100 mL Schlenk flask charged with 20 mL of toluene and $ZrCl_4$ (3.59 g, 15 mmol) was added dropwise a Li[$C_4H_3N(CH_2NMe_2)$-2] (6.00 g, 46 mmol)/toluene (20 mL) suspension at 0 °C with stirring. The resulting suspension was stirred for 3 h at room temperature and filtered through Celite. The residue was extracted with 20 mL of toluene in three portions and filtered through Celite again. The combined toluene filtrates were dried under vacuum, and the resulting solid was recrystallized from toluene to generate 7.63 g of final product. Yield: 73%. A crystal suitable for X-ray structure analysis was obtained from a saturated toluene solution standing at −20 °C. ^1H NMR ($CDCl_3$): 2.36 (s, 18H, N*Me*$_2$), 3.60 (s, 3H, C*H*$_a$N), 4.08 (s, 3H, C*H*$_b$N), 5.92 (m), 6.36 (m). ^1H NMR ($CDCl_3$, −60 °C): 2.03 (s, 9H, N*Me*$_2$), 2.69 (s, 9H, N*Me*$_2$) 3.57 (d, 3H, C*H*$_a$N), 4.12 (d, 3H, C*H*$_b$N), 5.92 (m), 6.36 (m). ^{13}C NMR ($CDCl_3$): 49.6 (q, J_{CH} = 142 Hz), 60.9 (t, J_{CH} = 145 Hz), 104.7 (d, J_{CH} = 166 Hz), 107.6 (d, J_{CH} = 167 Hz), 130.5 (d, J_{CH} = 182 Hz), 137.2 (s). Anal. Calcd for $C_{21}H_{33}ClN_6Zr$: C, 50.83; H, 6.70; N, 16.93. Found: C, 50.59; H, 6.29; N, 16.10.

Ethylene Polymerization Experiments. The polymerization reactions were performed in a Parr 300 mL stainless steel reactor. Solvent and MAO were loaded in the reactor in a glovebox and removed after sealed. The reactor then was purged with ethylene. After reaching the reaction temperature and pressure, catalyst was injected into the reactor. The polymerization was quenched after a period of time by the addition of acidic methanol. Polymer was isolated by filtration and washed with acidic methanol and dried under vacuum.

X-ray Structure Determination of Compounds 1 and 2. The crystal was mounted on a glass fiber using epoxy resin, transferred to a goniostat, and cooled to 150(1) K under liquid nitrogen vapor. Data were collected on a Bruker SMART CCD diffractometer with graphite-monochromated Mo Kα radiation with the radiation wavelength of 0.71073 Å. Structural determinations were made using the SHELXTL package of programs. The absolute structures for complexes **1** and **2** were obtained by calculating the Flack absolute structure parameter *x*; the true value of *x* is close to zero. A SADABS absorption correction was made. All refinements were carried out by full-matrix least squares using anisotropic displacement parameters for all non-hydrogen atoms. All the hydrogen atoms are calculated. The crystal data are summarized in Table 1.

Acknowledgment. We thank the National Science Council of Taiwan for the financial support and the National High Performance Computing Center of Taiwan for supporting the databank searching. We also thank Dr. Darin Tiedtke for helpful discussions.

Supporting Information Available: Crystallographic data for **1** and **2** and ^1H NMR spectra for all new compounds. This material is available free of charge via the Internet at http://pubs.acs.org.

OM010198B